SURF Threshold De-noising Method Based on the Contourlet Wavelet Transformation

Min Yuan[1], Hui Sheng[1,2]
1.Electronic Information Department, Information Engineering School, Yancheng Institute of Technology, Yancheng 224051, China
2.College English Department, Yancheng Institute of Technology, Yancheng 224051, China
E-mail: min_yuan0102@163.com

***Abstract*—Image noise always affects the clarity of the image and leads to blurring. However, the traditional de-noising methods cannot effectively remove the image noise especially the noise in regions contains rich detail information. In order to eliminate the noise, preserve better detail information of the images and enhance the de-noising effect of Contourlet wavelet transformation for images and curb pseudo Gibbs phenomenon, the paper combines SURF threshold method to improve the image processing effect. This paper improves Contourlet transformation method and develops interface, which effectively integrates it with SURF threshold and ensures the practical application. The paper also designs image de-noising experiment, which compares the result of processing with only Contourlet transformation method and that with Contourlet-SURF threshold transformation method and carries out PSNR evaluation. The results prove the effectiveness of Contourlet—SURF threshold transformation method's effectiveness, with pseudo Gibbs phenomenon being better curbed.**

***Index Terms*—wavelet analysis, contourlet method, surf threshold, image de-noising**

I. INTRODUCTION

The image noise generally refers to the remaining signal other than the desired signal. According to noise model, noise can be divided into the salt and pepper noise and Gaussian noise. The noise pulses generated from sensors and transmission channel in the digital image acquisition and transmission process which often produce the black and white points in the image are called salt and pepper noise [1]. The imaging system consists of many different linear subsystems. The image in the imaging process, each step will introduce noise and increases the uncertainty of the noise, referred to as random noise [2].The noise introduced in each step of the imaging process which increase the noise uncertainty is called random noise. With the rapid development of computer science and image processing technology, the digital image is widely used in medical imaging, pattern recognition, etc. Some scholars have put forth a lot of noise removal algorithms as realistically as possible to restore the original image. In order to simulate the objective objects studied, different types of noise often need to be artificially produced in the signal processing, in which the most common kind of random noise model is Gaussian white noise. Gaussian white noise widely used in image signal processing contains all frequency components and has the nature of the Gaussian distribution [3].

There are two kinds of traditional image de-noising methods: One is the processing for the whole image based on frequency domain, such as low-pass filtering, Wiener filter, Kalman filtering and so on [4, 5, 6]; The other is the local processing for the neighborhood of a pixel in the image based on the spatial domain [7], such as median filtering, statistical filtering and local adaptive filtering [8]. The frequency domain based methods are completed in the Fourier transform domain, which has good localization ability in the frequency domain, but does not have the analysis ability in the time domain, so the performance at any time point cannot be obtained [9]; The spatial domain based methods also have such problems. Therefore, these two types of de-noising processing is either in the frequency domain, or entirely in the spatial domain. Although noise is suppressed, image edge details are lost, which will blur the image.。 Image de-noising methods can be divided into linear filtering and nonlinear filtering according to the filter type. Linear filtering includes non-weighted neighborhood averaging filter, ultra-pixel smoothing [10]; Nonlinear filtering mainly contains median filtering, wavelet decomposition and reconstruction method and nonlinear wavelet transform threshold value method [11] [12] [13]. All of those are suitable for the smoothness of the signal, but ignores the details of the signal. If the parameters selected improperly, the dependence of which will cause image blur.

In order to eliminate the noise, preserve better detail information of the images and enhance the de-noising effect of Contourlet wavelet transformation for images and curb pseudo Gibbs phenomenon, the paper combines SURF threshold method to improve the image processing effect. This paper improves Contourlet transformation method and develops interface, which effectively integrates it with SURF threshold and ensures the practical application. The paper also designs image de-noising experiment, which compares the result of

doi:10.4304/jcp.8.11.2997-3003

processing with only Contourlet transformation method and that with Contourlet-SURF threshold transformation method and carries out PSNR evaluation. The results prove the effectiveness of Contourlet—SURF threshold transformation method's effectiveness, with pseudo Gibbs phenomenon being better curbed.

II. ANALYSIS OF GRAPHICS DE-NOISING PRINCIPLE

Image de-noising is the method achieving threshold processing to the transform coefficients, and can be divided into the hard threshold and soft threshold method. Hard threshold compares the absolute value of the wavelet coefficients of the signal with the threshold value, maintains the wavelet coefficients greater than threshold, sets the coefficients less than the threshold zero, and then reconstructs the signal according to the wavelet coefficients. Soft threshold changes the wavelet coefficient greater than the threshold value into the difference between the point and the threshold value.

The basic idea of the traditional image denoising algorithm can be attributed to: First, carry out secondary wavelet transform to the noisy signal $f(k)$, select the appropriate wavelet decomposition level j to get appropriate wavelet coefficients; Secondly, take the threshold value process to get wavelet coefficients $W_{j,k}$ and the estimated wavelet coefficients $\hat{W}_{j,k}$ in order to make the value of $\left\| \hat{W}_{j,k} - u_{j,k} \right\|$ as small as possible in which $u_{j,k}$ represents the wavelets transform coefficient of the original signal; Finally, use $\hat{W}_{j,k}$ to reconstruct the decomposed wavelets and obtain estimated signal value $\hat{f}(k)$ which represents de-noising image signal. To the observed image signal:

$$f(k) = s(k) + n(t) \tag{1}$$

$n(t)$ represents noise with σ^2 as its variance, and $s(k)$ is the original signal. After the wavelet decomposition of $f(k)$, there are larger wavelets coefficients $W_{j,k}$ corresponded to $s(k)$ on each scale at some special points while other position the values of $W_{j,k}$ are smaller. Noise in the image, the corresponding wavelet coefficients $W_{j,k}$ to noise $n(t)$ in the image in each wavelet scales are uniformly distributed, and the value is relatively small, at the same time as the scale increasing the amplitude is continuously decreasing.

$\lambda = \sigma\sqrt{2\log(N)}$, wherein N represent the length of the signal.

Hard-threshold method using the following formula:

$$\hat{W}_{j,k} = \begin{cases} W_{j,k} & |W_{j,k}| \geq \lambda \\ 0 & |W_{j,k}| < \lambda \end{cases} \tag{2}$$

Soft-threshold method using the following formula:

$$\hat{W}_{j,k} = \begin{cases} sign(W_{j,k}) \bullet (|W_{j,k}| - \lambda) & |W_{j,k}| \geq \lambda \\ 0 & |W_{j,k}| < \lambda \end{cases} \tag{3}$$

These two methods are relatively easy to achieve, in which the wavelet coefficients can quickly be obtained, and have been widely used in practical applications. However, there are some defects in these two algorithms. As it can be inferred from Figure 1, in the hard-threshold method, $\hat{W}_{j,k}$ is discontinuous at the threshold point λ, therefore the signal reconstructed from $\hat{W}_{j,k}$ method will be unstable; In the soft-threshold method, when $|W_{j,k}| > \lambda$ wavelet coefficient $\hat{W}_{j,k}$ and coefficient $W_{j,k}$ has a constant difference λ. With the increase in the scale of the wavelet decomposition, the wavelet coefficients of details on the edge of the smaller scales is small, so noise removal is likely to cause the loss of edge information.

According to the decomposition relationship between the Lipschitz exponent and wavelet transform [14], with the increase of the wavelet scale and wavelet coefficients, the wavelet coefficients of the noise is reduced. Neither of the threshold method considering this feature, the same threshold at different decomposing scale inevitably causes the elimination of edge signal coefficient which lead to the loss of edge information and blurring of the images. Therefore, this paper proposes a compromise algorithm, the fuzzy threshold de-noising algorithm based on wavelet transform.

III. SUPERIORITY ANALYSIS OF WAVELET TRANSFORM

The conventional image noise analysis uses Fourier transform methods[15], whose transform and inverse transform formula are shown in (4), (5)

$$F(\omega) = F[f(t)] = \int_{-\infty}^{\infty} f(t) e^{-i\omega t} dt \tag{4}$$

$$f(t) = F[F(\omega)] = \frac{1}{2\pi} \int_{-\infty}^{\infty} F(\omega) e^{i\omega t} d\omega \tag{5}$$

(4)(5)highlight the image overall transform, express the frequency domain and the time domain nature transformation. In order to make Fourier transform also applied in small areas, the following improvements are

made: assume that the unstable image signal remains stable in time domain with a very small window function. Then conduct a translation, so that it makes $f(t)g(t-\tau)$ indicate the stable signal range extending to different time domains. According to this principle, it could obtain frequency spectrums of images in different time domains.

Specifically, Fourier transform divides the pseudo stationary image signal into a plurality of time domain. Time domain is sufficiently small to ensure that the fine core stability. It analyzes these time domain signals and expresses the time domain signal frequency. Formula (6) refers to Fourier transform format of ΔR in time domain.

$$F(\omega,t)=\int_{\Delta R} f(t)\overline{g}(t-\tau)e^{-i\omega t}dt \qquad (6)$$

$\overline{g}(t)$ refers to the complex conjugate function. Formula (6) represents that with the changes of time τ, the frequency limited function $e^{-i\omega t}$ and the time limit function $g(t)$, the determined time domain by $g(t)$ follows the changes and translate along the timeline. Meanwhile, $f(t)$ continuously conducts twisting analysis. At the same time, the expansion of the signal $F(\omega,t)$ can expressed as a state in time domain $[\tau-\sigma,\tau+\sigma]$ and small frequency domain $[\omega-\varepsilon,\omega+\varepsilon]$.

Excessive σ and ε will cause function distortion. However, according to the Heisenberg uncertainty principle, $\varepsilon\sigma\geq\frac{1}{2}$, so in theory, ε and σ are not infinitesimal [16]. Then the Fourier transform will not be able to deal with non-stationary signals.

In 1984, the French radio engineer, Morlet, proposed wavelet transform. At the same time it opened up a new situation in the signal processing.

Assume function $\psi(t)\in L^1(R)\bigcap L^2(R)$ satisfies $\int_{-\infty}^{\infty}\psi(t)dt=0$. Here $\psi(t)$ is the basic wavelet. Assume a as distance parameter; b time parameter, and wavelet function can be expressed as

$$\psi_{a,b}(t)=\frac{1}{\sqrt{|a|}}\psi(\frac{t-b}{a}) \qquad (7)$$

Set the objective function $x(t)\in L^2(R)$, carry continuous wavelet transform on $x(t)$, and

$$WT_x(a,\tau)=\left\langle x(t),\psi_{a,b}(t)\right\rangle=\frac{1}{\sqrt{a}}\int_R x(t)\psi^*\left(\frac{t-\tau}{a}\right)dt \qquad (8)$$

As can be seen from the above analysis, wavelet transform overcomes the window scale, frequency change without coherence and other disadvantages. Compared to the Fourier transform, it could provide a time change-frequency window which changes with the frequency, thus highlighting the wavelet transform processing and analysis of the signal frequency.

IV. CONTOURLET TRANSFORM ANALYSIS

Wavelet Contourlet transform consists of two levels. The first level uses wavelet transform for multi-scale decomposition, thereby replacing Contourlet transform Laplace transform item; the second level uses directional filter bank (DFB) to deal with the high frequency signal experiencing multi-changes in the first stage so that it realizes vector decomposition and make signal anisotropic.

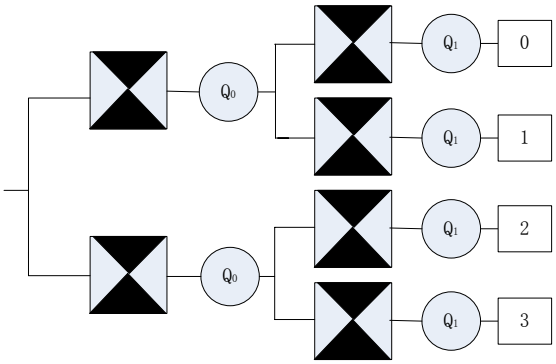

Figure 1. DFB Second Level Directional Filter Bank Wavelet Filtering

Figure 1 shows the two-stage processing of DFB. Q_0 and Q_1 are fan-shaped sample matrices. The implementation of sampling matrix plays a role in decomposing the first-stage image into horizontal and vertical directions; the employment of sampling matrix Q_1 takes effect in further decomposing the image processed in the first-stage and then output four sub-bands from 0 to 3, thus completing the image decomposition transformation in four directions. From the third stage, we first adopt R_0 - R_3 for re-sampling, and then conduct orientation filter and collect samples in Q_0 and Q_1 to finish decomposition. As R_0 - R_3 are shown in formula (9) and (10), the four sampling matrixes correspond to four different re-sampling methods. Resampling only gives rise to minor displacement of the pixel points under control. Besides,

the pixel position is reversible, and as a result the transformation does not affect the overall effect of the image.

As shown in Figure 1, the filter transformation of each layer in the secondary direction is realized through multi-scale decomposition by a discrete wavelet firstly so as to obtain a low frequency sub-band L and three high frequency sub-bands (a vertical sub-band LH , a horizontal sub-band HL , and a horizontal-vertical sub-band HH), and then focus on the processing of the three high-frequency sub-bands and directional decomposition of high frequency sub-bands with non-discrete directional filters of the same direction number. Here, L tree structure quincunx filter bank(QFB)is adopted as the directional filter. We can realize steering through the directional frequency decomposition and re-sampling. In this way, we can realize directional decomposition and decompose the image into 2^L directions.

$$Q_0 = \begin{pmatrix} 1 & -1 \\ -1 & 1 \end{pmatrix}, Q_1 = \begin{pmatrix} 1 & 1 \\ -1 & 1 \end{pmatrix} \quad (9)$$

$$R_0 = \begin{pmatrix} 1 & 1 \\ 0 & 1 \end{pmatrix}, \quad R_1 = \begin{pmatrix} 1 & -1 \\ 0 & 1 \end{pmatrix} \quad (10)$$

$$R_2 = \begin{pmatrix} 1 & 0 \\ 1 & 1 \end{pmatrix}, \quad R_3 = \begin{pmatrix} 1 & 0 \\ -1 & 1 \end{pmatrix} \quad (11)$$

l and the directional filter bank includes equivalent synthesis filter $G_k^{(l)}$ ($0 \le k < 2^l$) with 2^l directional sub-bands and the sampling matrix $S_k^{(l)}$ ($0 \le k < 2^l$). Figure 3 displays the multi-channel of the directional filter bank. The definition of sampling matrix $S_k^{(l)}$ is shown in formula (12).

$$S_k^{(l)} \begin{cases} \begin{bmatrix} 2^{l-1} & 0 \\ 0 & 2 \end{bmatrix}, 0 \le k < 2^{l-1} \\ \begin{bmatrix} 2 & 0 \\ 0 & 2^{l-1} \end{bmatrix}, 2^{l-1} \le k < 2^l \end{cases} \quad (12)$$

From formula (12), we can know that the sampling matrixes can be separated according to the limits, and these two sets are in accordance with the horizontal and vertical sets respectively. In this way ($g_k^{(l)}$) in $\left\{ g_k^{(l)} \left[n - S_k^{(l)} m \right] \right\}$ becomes the impact response of the synthesis filter $G_k^{(l)}$, and $0 \le k < 2^l$. $m \in Z^2$ makes up a set of directional base in the space of $l^2(Z^2)$.

In the orthogonal separable wavelet transformation, the discrete two-dimensional multi-resolution analysis is as follows:

$$V_j^2 = V_j \otimes V_j, V_{j-1}^2 = V_j^2 \otimes W_j^2 \quad (13)$$

Wherein the orthogonal complement space of the detailed signal of $W_j^2 V_j^2 V_{j-1}^2$ and the orthogonal basis of W_j^2 is $\{\Psi_{j,n}^1, \Psi_{j,n}^2, \Psi_{j,n}^3\}_{n \in Z^2}$. If we decompose the detailed signal l_j in the W_j^2 direction, we can obtain 2_j^l sub-bands of W_j^2 .

$$W_j^2 = \sum_{k=0}^{2^{l-1}} W_{j,k^l}^2 \quad (14)$$

Define

$$\eta_{j,k,n}^{i,(l)} = \sum_{m \in Z^2} g_k^j [m - S_k^{l_j} n] \Psi_{j,m}^i, i = 1,2,3 \quad (13)$$

$\{\eta_{j,k,n}^{1,(l)}, \eta_{j,k,n}^{2,(l)}, \eta_{j,k,n}^{3,(l)}\}_{n \in Z^2}$ is a set of orthogonal base of the subspace $W_{j,k}^{2,(l)}$. The above shows that wavelet Contourlet transformation is featured with multi-scale and multi-direction.

The wavelet Contourlet transform is non-redundant. Wavelet can indicate edge through capturing separated singular point, while Contourlet transformation is able to outline the edges of the image. Wavelet Contourlet transform possesses the approach ability of nonlinearity. Thus, it can realize better sparse representation of image.

V. SURF Threshold Improvement of Contourlet Transformation

The translational variability of Contourlet transformation will cause distortion among the discontinuous neighbor points in the process of de-noising of the noise, such as the pseudo-Gibbs phenomenon. The distortion position has something to do with the position of discontinuity point. The SURF threshold method is adopted to compensate for the deficiency of Contourlet Transform and curb the pseudo-Gibbs phenomenon.

Supposing N_i as Gaussion white noise, W_i as

the plus-noise image signal and S_i as the noise-free image signal in the ideal state, we can conclude it $W_i = S_i + \varepsilon N_i$, among which ε is the intensely controllable factor, and it submits to $N(0,\sigma^2)$.

The SURF transform threshold should be determined before the decomposed wavelet is dealt with. Priority should be given to solve the problem between the image variance and noise variance. For the noise σ_Y^2, there is the formula:

$$\sigma_Y^2(s,j) = \frac{1}{n^2(j)} \sum_{i,j=1}^{n(j)} N^2(i,j) \qquad (15)$$

Wherein, $N(i,j)$ obeys Gaussian distribution. The variance of the image is as follows:

$$\sigma_X(s,j) = \sqrt{\max(\sigma_Y^2(s,j) - \sigma^2(s,j), 0)} \quad (16)$$

According to formula (13), the best threshold obtained in formula (14) is:

$$T(s,j) = \begin{cases} \sigma^2(s,j) \Big/ \sigma_X(s,j), & \sigma_X(s,j) > 0 \\ \max(|N(s,j)|), & \sigma_X(s,j) \le 0 \end{cases} \qquad (17)$$

On the basis of determining the threshold, the decomposition levels of wavelet should be set.. With more levels, the transformation will decompose the low frequency more accurately with the resolution of the signal being higher accordingly. However, as the signals are decomposed gradually, it will be more difficult to handle it, while the effect is less obvious. There are 3 layers in this paper.

$$\Phi(x) = 2\sum_k \tilde{H}_k \Phi(2x-k) \qquad (18)$$

$$\Psi(x) = 2\sum_k \tilde{G}_k \Psi(2x-k) \qquad (19)$$

Using (18), (19) for wavelet reconstruction, in which $\tilde{H}_k$ and $\tilde{G}_k$ are called the inverse wavelet filtering matrix. After the reconstruction, wavelet de-noising is completed.

Image processing steps are as follows:

(1) Carry out wavelet Contourlet Transform on the image to get the Wavelet Contourlet coefficients of each scale and in all directions;

(2) Use formula (17) to estimate SURF threshold value of Wavelet Contourlet coefficients, and use Surf threshold function for threshold processing;

(3) Carry out inverse transform of wavelet Contourlet on coefficient of wavelet Contourlet after threshold processing;

(4) The results obtained by the step (3) is used for the second time in Surf threshold processing to obtain the de-noised image;

(5) Sum the de-noised image obtained by the step (4);

(6) The final de-noised image could be obtained after linear average of accumulated sum of step

VI. SIMULATION AND ANALYSIS OF THE IMPROVED CONTOURLET METHOD

All experiments of this article are carried out on the computer with PC P4 T2310 1.86G, 2GRAM, Inte182865G graphics cards. Experimental environment is MATLAB7.0. The experiments use two sets of images: 256 × 256 infrared images and Barbara image with gray level 256. De-noising is carried out according to the method set forth above on the two sets of images, Figure 2 and Figure 3.

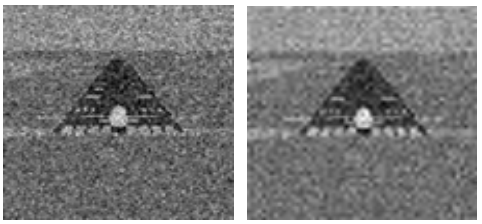

(a)Noise image (b)Wavelet transform method

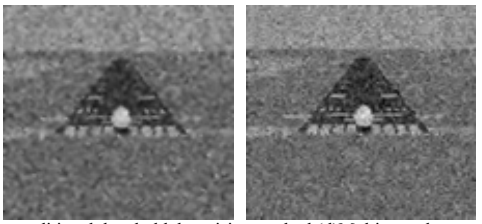

(C)The traditional threshold de-noising method (d)Multi-wavelet transform method

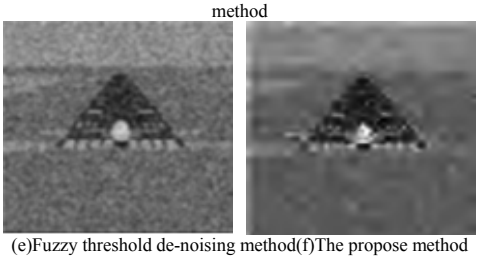

(e)Fuzzy threshold de-noising method(f)The propose method

Figure 2 Infrared image de-noising algorithm charts

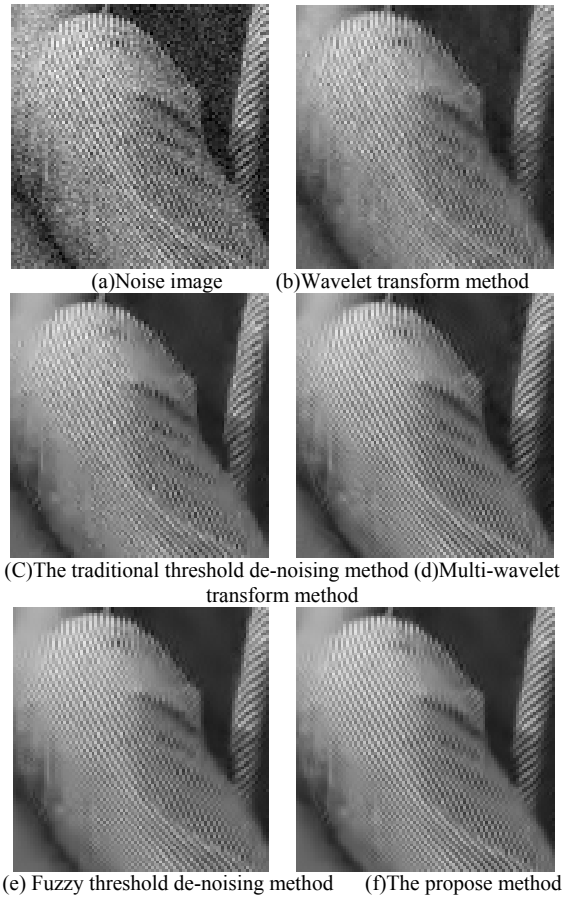

(a)Noise image (b)Wavelet transform method

(C)The traditional threshold de-noising method (d)Multi-wavelet transform method

(e) Fuzzy threshold de-noising method (f)The propose method

Figure 3 Barbara image de-noising algorithm charts

It can be inferred from Figures 2 and 3 that the improved algorithm in this paper has a better image edge and texture information recovery than traditional wavelet method, multi-wavelet method and fuzzy threshold method. The proposed algorithm can save rich texture and edge information of the image with a better subjective effect.

For further instruction of the superiority and practicality of the proposed algorithm, the image quality assessment is introduced in the paper. Image quality evaluation includes two aspects, one is the clarity of the image, and the other one is the readable degree. Here the clarity of the image describes the degree of deviation between the image evaluated and standard image, and the image readable ability expresses the readable information the image provide to person or machine. The present study found that non accurate assessment model of the human visual characteristics have been established to evaluate the clarity and the readable ability of the image, so the evaluation of image quality still exists a certain degree of subjectivity. Objective evaluations of image quality standard typically used are the standard of the peak signal-to-noise ratio (PSNR) and root mean square error (RMSE), which are defined as follows

$$PSNR = 10\log(\frac{\sum x^2(n)}{\sum[x(n)-\hat{x}(n)]^2})$$

$$RMSE = \sqrt{\frac{1}{n}\sum[x(n)-\hat{x}(n)]^2} \quad (20)$$

$x(n)$ and $\hat{x}(n)$ are the gray value and de-noising gray value of (m,n) th pixel of the image. Table 1 lists PSNR values of the various de-noising method, from which we can obtain that PSNR value of the proposed method are higher than other methods in a variety of noise intensity

TABLE 1

PSNR COMPARISON

Test image	σ noise imag	PSNR wavelet method	multi wavelet	traditional threshold	fuzzy threshold	proposed method
Infrared	8	28.14	33.70	35.14	35.18	35.19	35.33
	1	24.62	31.74	33.34	33.30	33.20	33.54
	2	22.15	30.18	32.10	31.95	31.84	32.23
	3	20.26	29.20	31.09	30.86	30.66	31.15
Barbara	8	28.15	31.38	33.16	34.00	33.96	34.50
	1	24.63	28.97	30.80	31.86	31.62	32.44
	2	22.16	27.47	29.10	30.31	29.89	30.79
	3	20.31	26.48	27.83	29.15	28.60	29.66

Image quality of Eyes image and Barbara image are very high. The proposed method is able to preserve better image edge information and not produce artifacts.

The noises can be controlled effectively by the method of Contourlet transformation, but the white noise phenomenon still remains with a lot of image sharp noise points. The improved Contourlet method is based on the filtering effect of SURF threshold value, so the noise in the signal is well suppressed, the processed signal is smooth, and the additional shock phenomenon is eliminated. The de-noising effect of the signal is very prominent, with the processing efficiency and application compatibility retained at the same time.

VII. CONCLUSION

The superiority of the wavelet transformation is reflected by analyzing the limits of Fourier transformation in processing the signal. This paper analyzes the principles of Contourlet wavelet transformation and establishes the Contourlet wavelet analysis model. Besides, the SURF threshold is introduced to improve the Contourlet transformation method. Finally, the paper designs the experiment to treat image of Lena for comparison and conducts PSNR analysis on the results. It is proved that the improved method can effectively suppress the pseudo-Gibbs and

uplift the reducibility and fidelity of the image.

VIII. REFERENCES:

[1] R. H. Chan, C. W. Ho, M. Nikolova, "Salt-and-pepper noise removal by median-type noise detectors and detail-preserving regularization", *IEEE Transactions on Image Processing,* vol. 4, NO. 10, 2005, pp. 1479-1485.

[2] E. R. Dougherty, "Random processes for image and signal processing", *SPIE Optical Engineering Press*, 1999.

[3] M. Nussbaum, "Asymptotic equivalence of density estimation and Gaussian white noise". *The Annals of Statistics*, 1996, pp. 2399-2430.

[4] D. Ahn, J. S. Park, C. S. Kim, J. Kim, Y. Qian, T. Itoh, "A design of the low-pass filter using the novel microstrip defected ground structure", *IEEE Transactions onMicrowave Theory and Techniques*, vol. 49, NO. 1, 2001, pp. 86-93.

[5] J. Chen, J. Benesty, Y. Huang, S. Doclo, "New insights into the noise reduction Wiener filter", *IEEE Transactions on Audio, Speech, and Language Processing,* vol.14, NO. 4, 2006, pp. 1218 - 1234

[6] R. Frühwirth, "Application of Kalman filtering to track and vertex fitting", Nuclear Instruments and Methods in Physics Research Section A: Accelerators, Spectrometers, Detectors and Associated Equipment, vol. 262, NO. 2, 1987, pp. 444-450.

[7] C. Kervrann, J. Boulanger, "Optimal spatial adaptation for patch-based image denoising", vol. 15, NO. 10, *IEEE Transactions on Image Processing,* 2006, pp. 2866-2878.

[8] A. Buades, B.Coll, J. M., Morel, "A review of image denoising algorithms, with a new one", *Multiscale Modeling & Simulation*, vol. 4, NO.2, 2005, pp. 490-530.

[9] J. L. Starck, E. J. Candès, D. L. Donoho, "The curvelet transform for image denoising", *IEEE Transactions on Image Processing*, vol. 11, NO.6, 2002, pp. 670-684.

[10] T. Kailath, "A view of three decades of linear filtering theory", *IEEE Transactions on Information Theory*, vol. 20, NO. 2, 1974, pp. 146-181.

[11] Y. Lee, S. Kassam, "Generalized median filtering and related nonlinear filtering techniques", *IEEE Transactions on Acoustics, Speech and Signal Processing*, vol. 33, NO. 3, 1985, pp. 672-683.

[12] L. Huiying, L. Sakari, H.Iiro, "A heart sound segmentation algorithm using wavelet decomposition and reconstruction". *Engineering in Medicine and Biology Society, Proceedings of the 19th Annual International Conference of the IEEE,* vol. 4, 1997, pp. 1630-1633.

[13] A. Chambolle, R. A. De Vore, N. Y. Lee, B.J. Lucier, "Nonlinear wavelet image processing: Variational problems, compression, and noise removal through wavelet shrinkage", *IEEE Transactions on Image Processing* , vol. 7, NO. 3, 1998, pp. 319-335.

[14] Y. Y. Tang, L. Yang, L. Feng, "Characterization and detection of edges by Lipschitz exponents and MASW wavelet transform", *14th International Conference on Pattern Recognition, IEEE*, vol. 2, 1998, pp. 1572-1574.

[15] M. Sonka, V. Hlavac, R. Boyle, "Image processing, analysis, and machine vision", 1999.

[16] P. Busch, T. Heinonen, P. Lahti, "Heisenberg's uncertainty principle", *Physics Reports*, vol, 452. No. 6, 2007, pp. 155-176.